Earth and Planetary Science Letters, 98 (1990) 287–302
Elsevier Science Publishers B.V., Amsterdam – Printed in The Netherlands

[MK]

Collection of microparticles at high balloon altitudes in the stratosphere

John P. Testa, Jr. [a], John R. Stephens [b], Walter W. Berg [c], Thomas A. Cahill [d], Takashi Onaka [e], Yoshikazu Nakada [e], James R. Arnold [a], Norman Fong [a] and Paul D. Sperry [c]

[a] *Department of Chemistry, B-017, University of California, San Diego, La Jolla, CA 92093 (U.S.A.)*
[b] *Tritium Science and Technology, Mail Stop C348, Los Alamos National Laboratory, Los Alamos, NM 87545 (U.S.A.)*
[c] *National Center for Atmospheric Research, Boulder, CO 80301 (U.S.A.)*
[d] *Crocker Nuclear Laboratory, University of California, Davis, CA 95616 (U.S.A.)*
[e] *Department of Astronomy, Faculty of Science, University of Tokyo, Bunkyo-ku, Tokyo 13 (Japan)*

Received September 28, 1989; revised version accepted February 15, 1990

We report the collection of stratospheric particles at 34–36 km using balloon-borne collectors. The concentration of particles on the collection surfaces and element concentrations were measured on the majority of the particles using scanning electron microscope (SEM) and proton-induced X-ray emission (PIXE) analysis respectively. Particle morphologies, elemental composition, and electron diffraction data were obtained on a small number of the collected particles using transmission electron microscope (TEM) techniques.

The concentration of particles between 0.045 (lower imaging limit) and 1 μm in radius is several orders of magnitude above the blank levels on the collection surfaces while the concentration of particles above 1 μm is near blank levels. More than 10^6 submicron particles were collected. The concentration of submicron particles is between 10 and 50 times the concentration expected at the sampling altitude based on models using the measured flux of extraterrestrial particles to the atmosphere. The higher concentration of submicron particles may be due to contributions from volcanic particles, inaccuracies in the influx of particles of this size to the earth, or breakup of larger particles.

Analysis of the elemental composition using PIXE showed Cl, S, Ti, Fe, Br, Ni, Zr, Zn, Sr, and Cu in decreasing order of concentration. Elements below S could not be detected in the analysis. Cl, S, and Br are believed to be present due to reaction of the collection surfaces and particles with atmospheric gases while the other elements are present in the particles. The elemental composition of the particles does not allow an unequivocal origin to be assigned because particles from several of the possible sources listed above contain the measured elements.

TEM analysis of 23 of the submicron particles showed 16 to be non-graphitic. The particles ranged from Al rich silicates to almost pure Fe to one containing almost exclusively Ba and S. None were definitely chondritic in composition.

This collection of particles complements existing collections obtained by aircraft. They were collected at much higher altitude and are predominantly submicron in size. Collection and analysis of particles at high altitudes using balloons presents unique challenges and opportunities in understanding the particle population in the stratosphere.

1. Introduction

Small particles, either solid or liquid, although ubiquitous, make up a tiny fraction of the earth's atmosphere, on the order of ten parts per billion by mass in the remote troposphere. Yet their impact on atmospheric properties is profound, dominating many aspects of radiation energy transfer and optical visibility, serving as a sink for natural and anthropogenic gases, and strongly influencing clouds and precipitation. These particles may be injected directly into the atmosphere from natural and man-made (i.e. primary particulate pollution) sources. Large volcanic eruptions can increase the number of particles at high altitudes [1–4]. Particles can also form from gas to particle transformations (secondary particles), for example, sulfur-rich particles are formed from gases in the so-called Junge layer. Finally, particles, especially those at high stratospheric altitudes, may include a significant extraterrestrial component [5]. The mass and composition of particles vary greatly as a function of time, location, and altitude.

Most of the small extraterrestrial particles that enter the earth's atmosphere vaporize at altitudes from 80 to 100 km, where atmospheric pressure is on the order of 10^{-5} atmospheres. Megie and

Blamont [6] have shown that this material remains in the vapor state for some time (on the order of days) before being removed by particle formation and settling. Turco et al. [7] and Toon et al. [8] have modeled the formation and turbulent mixing of particles in th stratosphere. They considered the chemical reactions relating to vapor formation and also the nucleation, condensation, and coagulation of the particles. Hunten et al. [9] extended their model with emphasis on the role of fine meteoritic particles in promoting the heterogeneous nucleation of sulfuric acid particles in the sulfate layer. In their model the meteoritic component dominates the particle size distribution in the sulfate layer for the smallest (< 0.5 μm) and the largest sizes (> 10 μm) with sulfate aerosols dominating in the middle size range (~ 1 μm).

The top of the sulfate layer is believed to be at about 33 km based on measurement of the concentration of negative ions [10,11]. Sulfate particles should not form or survive above 35 km because the vapor pressures of H_2SO_4 and HSO_3 at the higher temperatures above this altitude preclude sulfate aerosol formation. Above the sulfate layer the extraterrestrial particles, together with particles injected by episodic volcanic activity, are believed to be the predominant particle populations. Below the sulfate layer substantial mixing with tropospheric air introduces an overwhelming concentration of suspended dust which dominates the particle population.

Collection of particles in the stratosphere has been carried out for many years [12,13]. Altitudes up to about 20 km are accessible using high-altitude aircraft such as the Lockheed U-2. Aircraft collections of small particles have provided us with micron and larger sized particles that include samples of unaltered micrometeoroids, presumably mainly of cometary origin, volcanic particles, and Al_2O_3 particles produced from solid state rocket motors. Al_2O_3 particles are the most abundant at aircraft collection altitudes.

Moderate-size balloons can be used for particle collections up to about 30 km. Collection of particle samples in the sulfate layer and above is difficult, although particle collection in the layer has been reported by Rosen and Hofmann [14]. Particles in the sulfate layer are predominantly sulfur-rich but some of the particles contain submicron cores of solid particles whose elemental composition suggests a non-terrestrial origin [9]. Above 30 km extended stays for stratospheric sampling can only be accomplished using large balloons. Because of the expected, very low concentration of particles, collection of stratospheric particles using balloons is not routinely attempted.

Collecting particles above the sulfate layer is important for several reasons. An unbiased collection of particles in the high stratosphere will give a good indication of the relative populations of particles of volcanic and extraterrestrial origin at a given time. Data on the evolution of volcanic particles may help us to understand stratospheric structure and mixing. Collection of extraterrestrial particles will complement the existing collections of particles now obtained at lower altitudes.

Particles at balloon altitudes are expected to consist of small (< 0.1 μm) particles formed in the stratosphere and micrometeoroids (> 1 μm) that have long stratospheric residence times. Particles formed in the stratosphere by the condensation of meteoric vapors condense at pressures of the same order as those postulated to have existed in the early solar nebula. Since no laboratory simulation can be carried out under such conditions (absence of wall effects) to study the condensation of grains, analyzing the stratospheric particles collected at high altitude may give us insights into the processes that formed particles in the early solar nebula. The earth's atmosphere is of course far more oxidizing than the early solar nebula, but the slow condensation and agglomeration of grains at low pressure makes the stratosphere a uniquely applicable model system.

We report here the results of a successful collection of stratospheric particles in May, 1985 at 34–36 km altitude. The particles were collected using a combination of cascade impactors and filters lofted by a large helium balloon. Particle concentration, particle size distribution, and bulk elemental composition were measured on a major portion of the collected particles using scanning electron microscope (SEM) and proton-induced X-ray emission (PIXE) instruments. Detailed particle morphology, elemental analysis, and electron diffraction data were obtained on 23 particles using a transmission electron microscope (TEM). The data are compared with the particle size distribution and concentration predicted to occur at these altitudes. Comparison of the elemental and

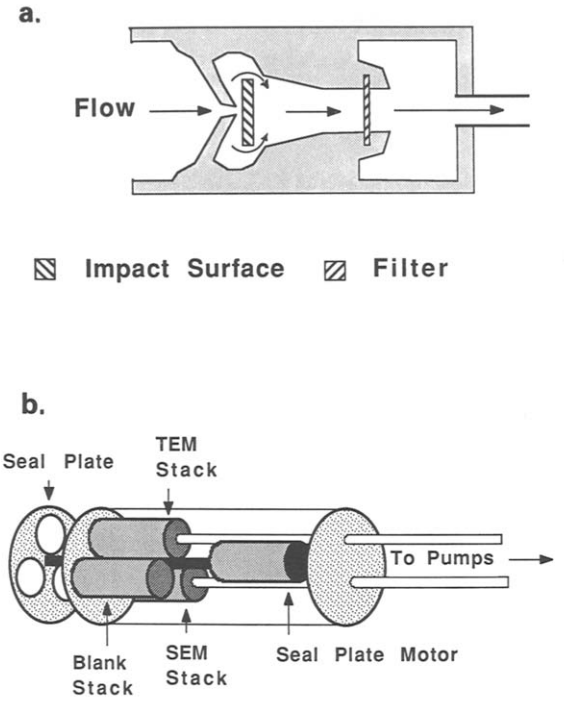

Fig. 1. Schematic of (a) an impactor stack showing the impact and filter surfaces and (b) the Cosmic Dust Collector used to collect stratospheric particles.

morphological data with characteristics of known extraterrestrial and volcanic particles is made in an attempt to deduce the origin of the collected particles.

2. Experimental

The apparatus used to collect the particles consists of a number of "stacks" each composed of a single stage impactor followed by a filter, a schematic of which is shown in Fig. 1a. Each stack contains a "Battelle" [15] impactor with a 2.63 mm diameter jet that impacts onto a 25 mm diameter Nuclepore Membrane Filter (NMF), referred to as an impact surface, followed by a 0.2 μm pore size NMF used as a filter. Because of the low pressure at the collection altitude the impactor does not produce a sharp size cutoff as it does at sea level; we used the impactor simply to concentrate the particles in a small area on the impact surface.

We measured the collection efficiency of an impactor/filter stack in the laboratory with the stack operating at the expected pressure (4 mb) and temperature ($-35\,^{\circ}$C) Particles of Yb with a particle diameter less than 0.5 μm were generated thermally in argon gas. Approximately 75% of the particles generated were retained on the NMF impact surface, mostly concentrated under the jet near the center of the NMF.

Three stacks were used in the flight instrument. One stack, referred to as the "SEM stack", used NMF's for both the impact surface and filter. The impact surface of a second "TEM stack", used to collect particles for TEM analysis, consisted of nine beryllium TEM grids, coated with "holey" carbon film, glued to a NMF impact surface in a cross pattern followed by a NMF used as a filter. A third "flight blank" stack was configured like the SEM stack but was not attached to a pump and hence received no flow during the flight.

To minimize handling after the flight the surfaces were prepared so that they could be inserted directly into the instrument to be used for analysis. All of the NMF surfaces were coated with silver prior to the flight to enhance the image contrast and reduce sample charging in the SEM while counting particles. We used silver because the M X-ray lines of gold in the gold-palladium coating normally used for SEM imaging interfere with sulfur L X-ray lines from the samples. No grease or oil was used to enhance particle retention on any of the surfaces because such coatings would interfere with the planned analyses.

The preparation and handling of the impact surfaces and filters took place in a still box under a laminar flow hood inside an enclosed work area. All work done prior to the post-flight measurements was done in a clean work environment. Workers wore standard clean room garments and gloves.

The collection stacks were installed in a sealed stainless steel housing "Cosmic Dust Collector" a schematic of which is shown in Fig. 1b. The Cosmic Dust Collector was integrated with a payload developed at the National Center for Atmospheric Research (NCAR). The two sampling stacks were plumbed to separate liquid nitrogen cooled molecular sieve sorption pumps in the flight payload. The stacks were sealed by a plate that was opened for sampling at altitude and then closed under automatic control. The payload included instruments to measure ambient pressure and flow rates as well as to monitor internal and

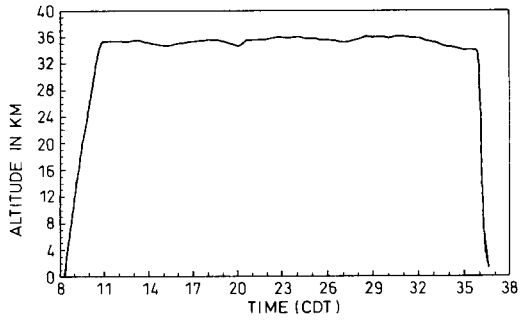

Fig. 2. Altitude–time profile.

external temperatures. All data was transmitted to a mobile ground station for recording.

Full configuration tests of the NCAR payload, including the Cosmic Dust Collector, were carried out at Holloman Air Force Base in Alamagordo, New Mexico using their environmental chamber which has both pressure and temperature control. Calibration of flow measurements used on the flight were performed at Holloman by measuring the pressure differential between the ambient chamber pressure and the pressure at the pump head (ΔP) in the payload as a function of mass flow into each collector stack, measured using a mass flow meter.

The balloon flight took place from Palestine, Texas in May 1985. The flight allowed 25 h of sampling between 34 and 36 km altitude, somewhat lower than intended. Figure 2 shows the altitude–time profile. The integrated flow measurements for the SEM stack, via the calibrated ΔP data, correspond to 160 l of air at STP. The actual volume sampled was 24.5 m^3 (+/− 20%). Flow measurements for the TEM stack were off-scale throughout most of the flight and could not be used to derive a sampled volume.

After recovery the Cosmic Dust Collector was removed from the flight payload and returned to San Diego where it was dismantled. The two collection stacks and the flight blank stack were disassembled in the clean room. The impact surfaces showed a yellowish-brown discoloration below the jet where the maximum flow occurred while the blank impact surface showed no discoloration. The discoloration is believed to be due to reactions of atmospheric Cl and Br with the Ag coating on the impact surfaces.

The collection surfaces and the blanks were studied using several instruments. A Cambridge S4 Scanning Electron Microscope (SEM) at the University of California, San Diego (UCSD) was used to count particles and to obtain qualitative energy dispersive X-ray data. The flight TEM grids were analyzed in the transmission mode using a Philips 400 TEM located at the Facility for High Resolution Electron Microscopy at Arizona State University. PIXE analysis of the flight samples was accomplished using the accelerator at the Crocker Nuclear Laboratory at the University of California, Davis.

3. Results

3.1. SEM particle counts

The numbers of particles on the impact and filter surfaces for all three flight stacks were measured using a SEM. Energy Dispersive X-ray (EDS) data were collected while images for particle counts were being obtained. Sulfur and chlorine were the predominant elements present but peaks of silicon, magnesium, aluminium, and iron were also identified. The resolution of the instrument allowed us to see particles down to 0.045 μm radius with confidence.

We made a random pattern search of the SEM impact surface and also followed a radial track from near the center out to the edge of the surface. The flight filters and flight blank surfaces were investigated based on a randomly generated pattern. The statistical uncertainties in the figures are based on the actual number of particles counted in each area.

Average particle concentrations on the flight blank filter and impact surfaces as well as the concentration on several handling blanks are shown in Fig. 3. For the flight blanks only upper limits to the particle concentrations could be established in some size bins because no particles were found. The average handling blank is derived from two blanks that were run in parallel with the flight surfaces, including traveling to Palestine and back, and two surfaces that were flown during an unsuccessful flight in 1984. In the unsuccessful flight the balloon ruptured at the tropopause and the surfaces remained sealed.

Figure 4 shows the average particle concentrations on the SEM impactor and filter surfaces as

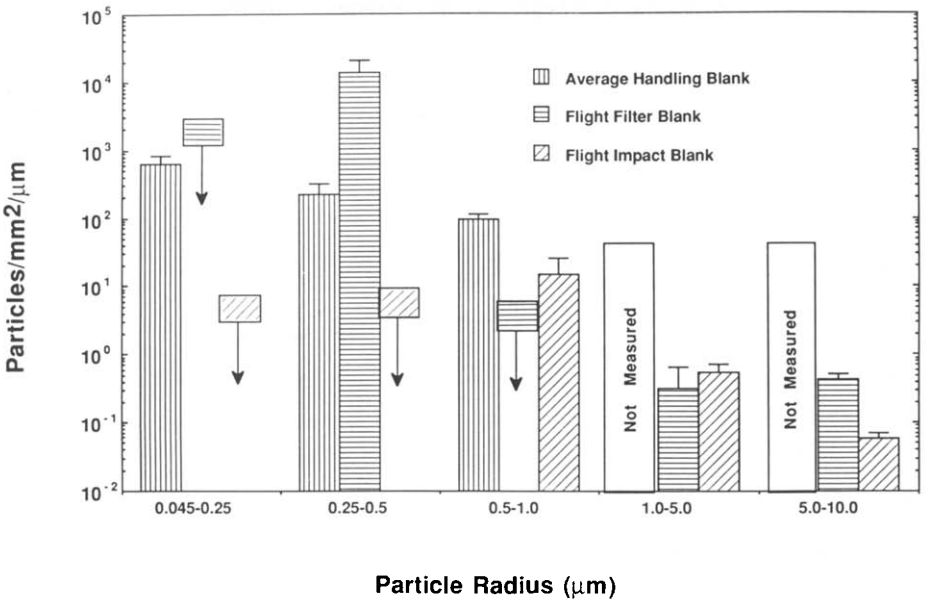

Fig. 3. Particle concentrations on handling blanks and flight blank surfaces. Upper limits in some bins, indicated by arrows, occur because no particles were counted in those size bins.

well as the concentration of particles in the 2 mm radius center of the impact surface immediately below the jet. For particle radii below 1 μm, the average impact surface concentration was 5–10 times the concentration on the filter surface, with the center of the impact surface showing con-

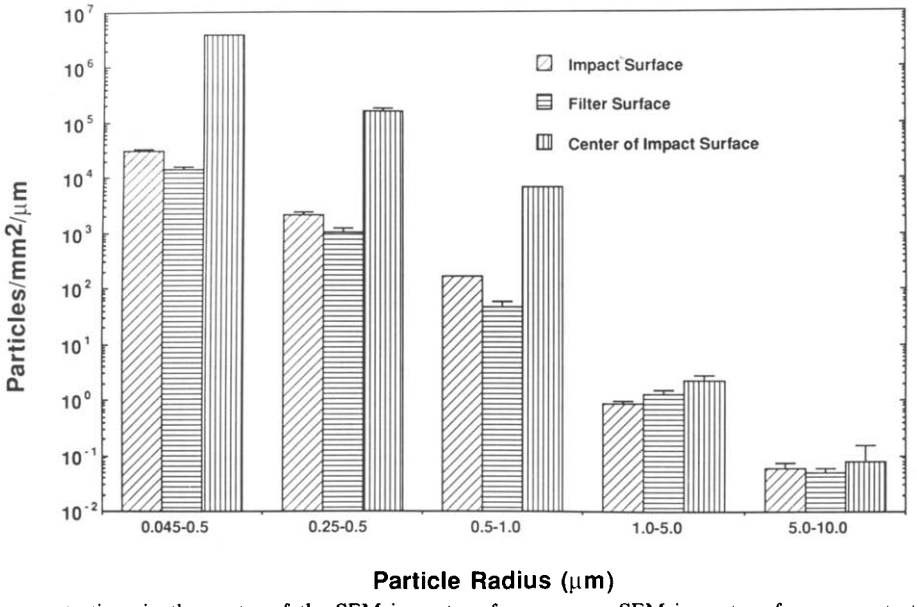

Fig. 4. Particle concentrations in the center of the SEM impact surface, average SEM impact surface concentration, and average concentration on the SEM filter surface. Particle concentrations were uniform on the filter surface but were sharply peaked in the center of the impact surface.

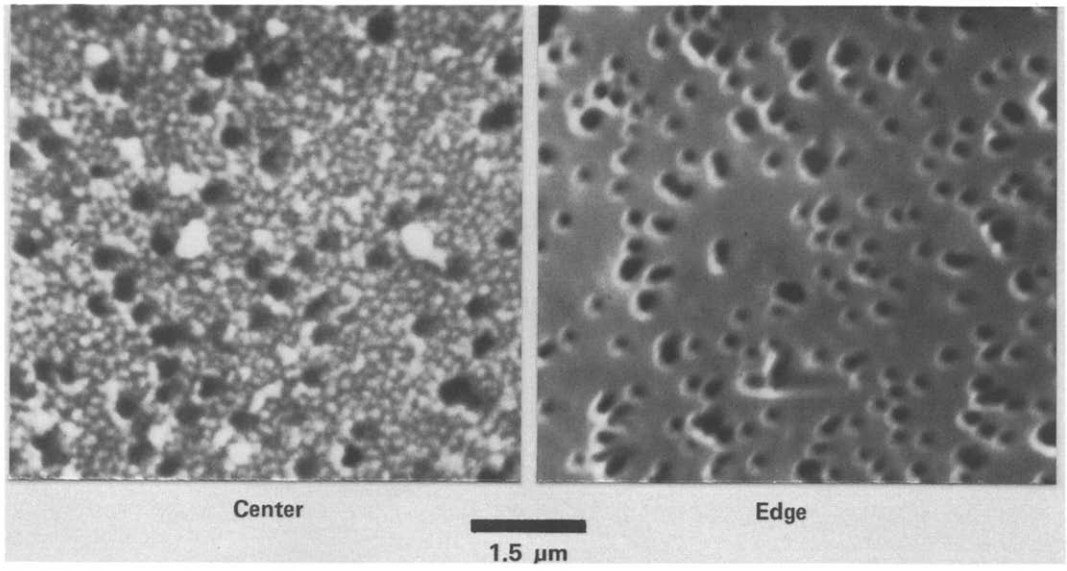

Fig. 5. Scanning electron micrographs of the center and edge of the SEM impact surface. The holes in the surfaces appear black while the particles appear white. The concentration of particles at edge of the impact surface is close to blank levels.

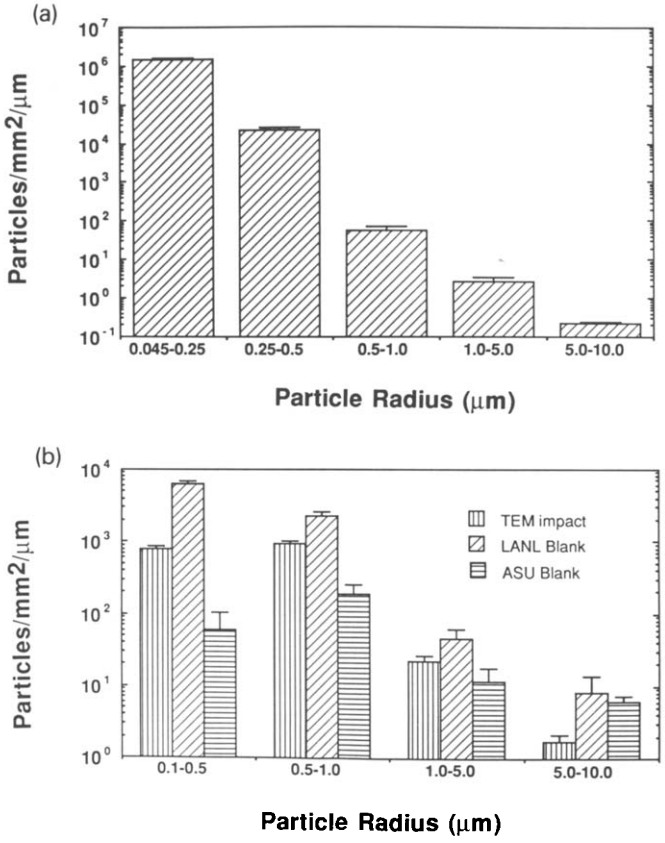

Fig. 6. Particle concentrations on (a) the TEM filter surface, and (b) the TEM flight impact grids and blank grids. Concentrations on the filter surface were measured using a SEM.

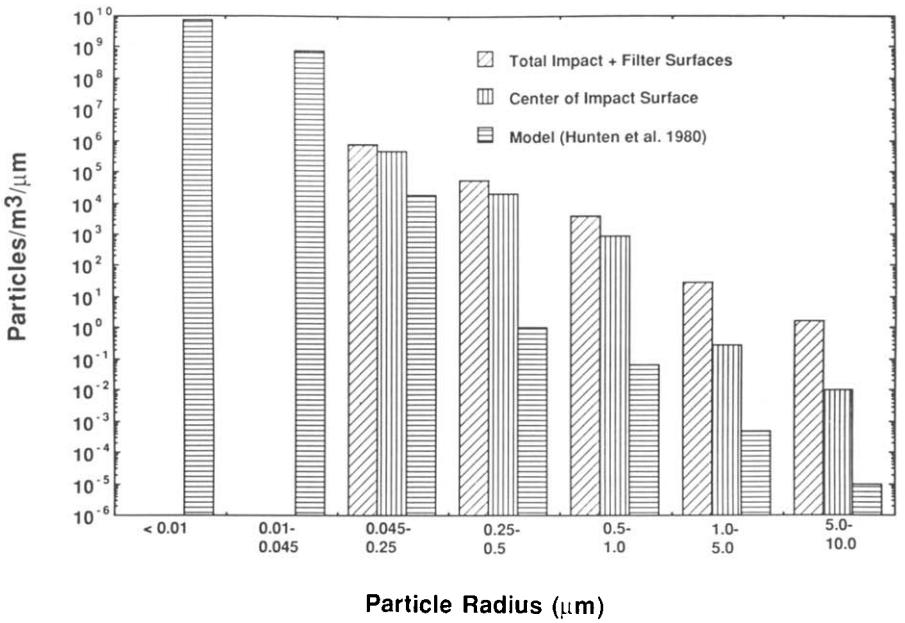

Fig. 7. Derived particles concentrations at the 35 km collection altitude based on the total particles collected on the SEM impact + filter surfaces and center of the SEM impact surface relative to the concentrations predicted by Hunten et al. [9]. Sizes greater than 1 μm radius contain substantial contributions from contaminating particles.

centrations at least a factor of 100 larger than the filter surface. For particles larger than 1 μm, the concentrations of particles are within a factor of three for the three areas. The average concentration of particles on the SEM impact and filter surfaces are $>$ 5 times the concentration on the blanks for particles smaller than 1 μm except for the 0.25–0.5 μm size bin of the flight filter blank. For particles larger than 1 μm, the collected particle concentrations are similar to the blanks. The concentrations of particles in the center area of the impact surface is $>$ 20 times that on the blanks for particles below 1 μm in radius, with concentrations similar to the blanks for larger sizes.

The difference in particle concentration between the center and the edge of the SEM impact surface is shown in Fig. 5. The black areas are the 0.2 μm diameter holes in the NMF. The particles appear white. The mottled white appearance of the filter may be due to a combination of many small particles and inhomogeneities in the silver coating on the filter. There can be no doubt that, at least in the center of the impact surface, numbers of stratospheric particles were collected.

The particle concentrations on grids on the TEM impact surface and on the TEM filter surface are shown in Fig. 6 together with the concentration of particles on several blank grids. The "LANL Blank" is a grid that was flown on the unsuccessful flight in 1984. The "ASU Blank" was handled in parallel with the flight surfaces but did not fly. For all particle sizes, the flight TEM grids showed concentrations similar to those of the blanks. Most of the particles on the blank TEM grids were identified as poorly graphitized carbon based on their unique morphology and lack of X-ray spectra [16]. Poorly graphitized carbon particles are produced as a by-product of depositing carbon films on the TEM grids. Seven of the 23 particles from the flight TEM grids were also identified as poorly graphitized carbon.

The TEM filter surface showed particle concentrations several orders of magnitude greater than either the TEM grid blanks or the flight impact blank for the smallest particle size bin below 0.5 μm. Particle concentrations for larger sizes were within an order of magnitude of the flight impact blank. In contrast to the SEM stack, in which the impact surface retained most of the

particles, in the TEM stack most of the particles were retained on the filter surface. We believe that the TEM grids, glued to the impact surface, disturbed the flow below the jet leading to low particle collection efficiency. Unfortunately, we do not know the flow through the TEM stack because the ΔP measurements, from which the flow is derived, were off scale for most of the flight due to either a malfunction of the instrument or to a high flow rate (though the latter seems excluded because of the flow impedance of the piping). Because of the uncertainty in the TEM particle counts and flow we used particle counts from the SEM stack to derive the concentration of particles in the stratosphere.

Figure 7 shows a comparison between the concentration of particles at the sampling altitude, derived from our flight data, and the predicted particle concentrations from the model of Hunten et al. [9]. Shown are both the number of particles on the center 2 mm of the impact surface and the total number of particles on the impact plus filter surfaces in the SEM stack. We believe that the number in the central area most accurately represents the true concentration of particles at the collection altitude.

The concentration of particles we collected is similar to the concentrations measured using and concentrations derived from balloon and satellite instrument data. Osborn et al. [24] reported particle concentrations measured from balloons, LIDAR, and SAGE II satellite extinction data obtained over the period November 29, 1984–October 11, 1986. The various measurements were performed as part of a correlative study to validate and calibrate satellite extinction data. Satellite, LIDAR, and balloon particle concentrations agree within the measurement uncertainties above 15 km altitude. LIDAR data extend only up to 29 km.

The balloon data, covering the period December, 1984–July, 1986 at Laramie, Wyoming and Fairbanks, Alaska, all showed the same concentrations of particles at 35 km. A balloon flight from Yuma, Arizona on May 15, 1985 showed essentially the same concentration of particles at 35 km (Rosen, pers. commun.). Particle concentrations at 35 km, measured using an optical particle counter which measures total particle concentration above 0.01 μm, averaged 2×10^6 m^{-3}. Our measured concentration of particles greater than 0.04 μm radius is 1×10^5 m^{-3}. Because the balloon data extend to smaller particle sizes, the measured particle concentration is expected to be greater than our measurements. Given the uncertainties in the measurements, the agreement between our collections and the balloon data is quite good.

Our particle concentrations also correlated well with satellite extinction data measured using the SAGE II instrument. Wang et al. [25] report particle concentrations derived from SAGE II extinction data from November 30, 1984. Assuming either a lognormal or a modified gamma size distribution, they derived particle concentrations up to 25.5 km altitude. Using their size distribution at 25.5 km and their extinction data, which extends to 35.5 km, we derive a total particle concentration at 35 km of 4.2×10^4 m^{-3} for particle sizes between 0.05 and 1 μm, in substantial agreement with our data, given the uncertainties in both. Direct inversion of multiwavelength SAGE II extinction data reported by Livingston and Russell [26] for a Brazil sunrise event on April 6, 1985 yields a total particle volume of 8×10^{-3} $\mu m^3/cm^3$ which is, within the uncertainty, the same as the particle volume derived from our data, 7×10^{-3} $\mu m^{-3}/cm^3$.

A referee has suggested that the particles, though collected in the stratosphere and not seen on blanks, may be derived from the balloon-gondola system rather than from natural sources. The balloon, located 500 m above the gondola, could only transfer particles in the total absence of wind shear. We shared the gondola only with an NCAR trace gas experiment, also with strict cleanliness requirements. Most important, submicron particles are well-known to be difficult to transfer from one surface to another, because of the dominance of surface forces (see, e.g. [28]).

We conclude that the particles collected during our flight were actually present in the stratosphere at the time of collection and are not contaminants. The similarity of particle concentrations derived from satellite and balloon data over large temporal and spatial scales suggest that the particle concentrations at 35 km do not vary rapidly. Comparing our collected particle concentrations with satellite data and balloon particle counting data taken at slightly different times and locations appears to be a valid procedure.

TABLE 1

Elemental composition of particles (%)

Particle no.	Na	Mg	Al	S	Ca	Fe	Ni	Other
Si = 100; elements > 1								
1	0	29	26	29	0	2	0	Cu-52, Mn-4, P-74 Cl-11
2	0	4	57	0	3	1	0	Cu-5
4	14	5	38	0	1	2	3	P-5, Zn-1
8	3	1	89	0	50	1	0	–
9	0	35	0	1	55	13	0	–
10	0	66	4	1	1	27	0	Cr-1
11	0	0	2	0	0	0	1	–
14	1	51	11	2	0	2	11	Zn-2
16	37	0	82	0	43	45	0	–
18	3	2	88	0	49	2	1	Zn-1
19	2	49	14	0	14	20	1	P-1, Sn-13
20	0	0	59	483	29	4	19	P-6, Cl-4, Cu-20, Ba-539, Zn-14
21	1	67	5	1	2	25	1	Cr-1
22	0	33	37	18	1	791	1	P-4, Cu-7, Pb-23
23	32	54	8	0	8	84	0	P-5, Cu-9, Cr-10
Without Si								
17	0	0	0	5	0	94	0	1% Mn

3.2. Morphology, elemental analysis, and diffraction data using TEM

Due to time constraints, only twenty-three individual particles on the TEM impact surface grids were examined. Of the 23 particles examined, 16 were identified as non-graphitic. We obtained electron micrographs, electron diffraction data, and energy dispersive X-ray spectra of the particles.

Elemental concentrations in the particles were calculated from the raw X-ray data using a Tracor Northern Standardless Metallurgical Thin Film Program. A background spectrum from a particle-free section of the carbon film on a TEM grid was subtracted from each particle spectrum after scaling the two spectra in flat regions of the spectra. The elemental ratio to silicon was then calculated using the appropriate microscope parameters including accelerating voltage, Be window thickness, Si detector dead layer thickness, and Au film thickness on the detector. Because the particles are small we assumed no X-ray absorption correction is required.

A summary of the elemental analysis of the non-graphitic particles is shown in Fig. 8 where we have plotted the relative Mg, Fe, and Si concentrations on a ternary graph. The symbols give the range of concentration of Al, relative to Mg and Fe, in the particles. Also plotted in Fig. 8 are the regions where stratospheric particles collected using aircraft, deep sea spherules, chondritic, crustal, and volcanic materials lie in the ternary

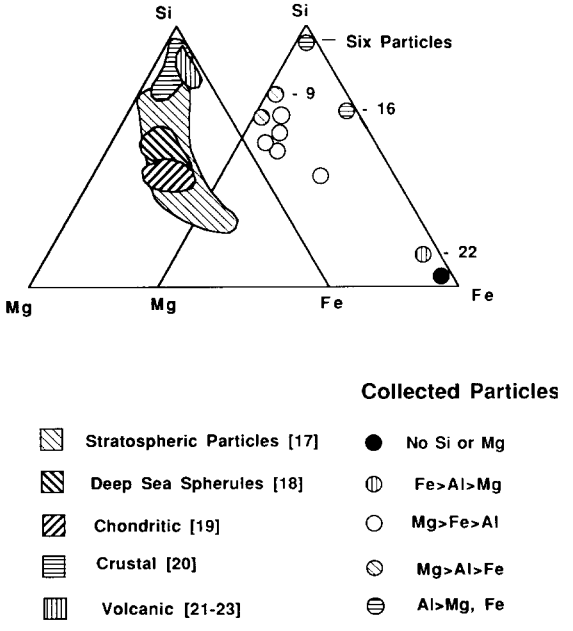

Fig. 8. Ternary graphs showing the relative Mg/Fe/Si concentrations in collected particles together with the composition of various classes of terrestrial and extraterrestrial particles.

diagram. Details of the elemental composition of the measured particles are given in Table 1.

Electron diffraction patterns of several of the particles were obtained while surveying the particles with the TEM. Ten of the resulting diffraction patterns yielded enough information to provide a tentative (but not unique) identification of the mineral phases in individual particles. The possible phases ranged from troilite ($Fe_{1-x}S$) in one particle (no. 22) with very high iron content to augite, Ca(Fe, Mg)SiO_6, in particle no. 9. Electron micrographs of three representative particles, 16, 9, and 22, together with electron diffraction data and possible phase identifications, are shown in Fig. 8.

3.3. PIXE analysis

The SEM impact and filter surfaces and also the flight blank surfaces were analyzed using proton-induced X-ray emission (PIXE) at University of California, Davis. The instrument has been used extensively for elemental analysis of tropospheric dust [27]. The silver coating on the NMF collection surfaces caused serious problems in analyzing the elements below S because the peak and low-energy tail of the Ag X-ray lines overlap the X-ray lines for low-Z elements. In addition a low-Z filter, which absorbs the X-ray lines below P, was left in place during the analysis of our samples. Only elements above S could be detected successfully.

The 2 mm by 3 mm PIXE beam was centered on the SEM impact surface. Since 94% of the mass of the particles in the center 2 mm radius of the impact surface consists of submicron particles we believe that the PIXE analysis provides an accurate elemental analysis of the collected stratospheric particles, except for S and Cl. The edge of the SEM impact surface and the flight blank showed signals substantially free of characteristic X-ray lines. We used the edge of the SEM impact surface as a blank to reduce the errors caused by changing samples during the analysis. The sample data were compared to elemental and mineral standards. A sensitivity level of 1 ng/cm^2 was achieved in the analysis. The elemental concentrations in the analyzed area are shown in Table 2.

TABLE 2

Elemental concentration on center of SEM impact surface by PIXE analysis

Element	Concentration above blank (ng/cm^2)
S	372 ±200
Cl	743 ±200
Ti	45 ± 15
Fe	5.6± 2.2
Ni	3.0± 1.0
Cu	1.4± 1.4
Zn	2.0± 1.0
Br	5.4± 1.5
Sr	1.5± 1.3
Zr	2.3± 2.1

4. Discussion

4.1. Particle concentrations

Large numbers of stratospheric particles have been collected particularly in the center of the SEM impact surface. The center area contains 62% of all of the particles collected in the SEM stack. The size distribution in the center area is strongly skewed toward submicron sizes. Particles greater than 1 μm represent only 10^{-4} of the total number of particles in the center area.

For submicron particles, stratospheric number concentrations, derived from our data, ranged from 10 to 10^5 times greater than the model of Hunten et al. [9], but are in reasonable agreement with other observations. Above 1 μm contamination prevents the derivation of reliable concentrations.

The total mass collected on the SEM impact and filter surfaces was estimated to be 218 ng. In the center area particles less than 1 μm make up 94% of the 28 ng total particle mass in this area. Since the center area of the SEM impact surface is the least affected by contamination, we will use particle counts from this area in the discussions below.

The total mass of submicron particles in the center of the impact surface is similar to the mass (31 ng) of meteoric particles according to the model of Hunten et al. [9]. The model however predicts that 96% of the particle mass is below 0.05 μm in radius with the mass concentration peaking at 0.02 μm radius, below our present imaging capabilities. Essentially all of the particles below 0.1 μm in the model are recondensed from meteoric vapors. Their size distribution is dependent on the nucleation, growth, and coagulation

assumed. Above 0.1 μm the particles are predominantly micrometeoroids that survive their passage through the atmosphere intact.

There are several possible explanations for the discrepancy between the collected and predicted concentration of particles. If few stratospheric particles exist below our lower detection limit of 0.045 μm the similarity in mass between our collected particles and the model predictions suggests that the average particle flux to the atmosphere assumed in the model accurately represents the local concentration of stratospheric particles, but that particle formation and growth is much faster and settling is slower than predicted. In the model the growth and coagulation of particles from the vapor are based on coagulation kernels by Fuchs [28] who assumes that growing particles are compact and have unity sticking coefficient. Recent work on coagulation, including numerical simulations, indicate that particles coagulate into open fluffy structures, sometimes described as fractals [29,30]. Such loose aggregates grow much faster than compact particles and should have much slower settling rates. More rapid growth by coagulation would shift the resulting particles to the larger size ranges (0.045–1 μm) where we can resolve the particles. Unfortunately particle morphologies are not well resolved in our counting studies. We do see some indication of loose aggregates. Several particles exposed to the focused beam in the SEM while obtaining EDS data broke up into many smaller particles that were near the resolution limit of the SEM.

There is also some indication that at least larger stratospheric particles collected by aircraft consist of loose aggregates of angular shards. Mackinnon et al. [31] examined all of the particles from a collection flag from an aircraft flight intended to sample the stratosphere after the El Chichon event and found that many of the particles consisted of loose clusters of grains. The concentration of grain clusters at the collection altitude was much greater than predicted if one assumed settling rates for spherical grains. More analysis of our particles is needed at higher spatial resolution to measure the concentration of particles smaller than 0.045 μm and study their morphology.

If the collected particles between 0.045 and 1 μm are not large recondensed particles the stratospheric particle number concentration is orders of magnitude larger than the micrometeoroid influx used by Hunten et al. [9] would predict. Several possibilities exist. The first is that there was a significantly higher concentration of extraterrestrial particles at our sampling location than that derived from the model. Higher local particle concentrations have been observed using LIDAR and ascribed to cometary particles [32]. More collection flights are necessary to resolve this issue.

A second possibility is that the population of particles impacting the stratosphere in the 0.045–1 μm size range may be larger than predicted, even if the average total mass of particles entering the stratosphere is accurate. The most significant particle mass impacting the atmosphere is believed to be about 10 μg or 100 μm in radius [9]. The concentration of particles smaller than 1 μm is very poorly known since their contribution to the total mass is small. If our particles are micrometeoroids, the micrometeoroid flux is much larger than previously thought. A larger flux of submicron micrometeoroids is in accord with particle counts by Zolensky and Mackinnon [33] in their survey of all particles found on a aircraft collection flag on which particle concentrations down to the lower size collection limit (~ 1 μm) were at least 10 times the concentration previously thought.

Another possible source of submicron particles is the breakup of larger porous micrometeoroids composed of low strength aggregates of submicron grains. Hunten et al. [9] included only vaporization of refractory micrometeoroids without breakup. Hawkes and Jones [34] in modeling the interaction of micrometeoroids with the stratosphere argue that breakup of porous aggregates is very likely when the material holding together the submicron grains in the aggregate is heated during atmospheric entry. A major class of interplanetary dust particles (IDP's) collected by aircraft in the lower stratosphere consist of porous aggregates of submicron grains that are easily broken apart [35]. Breakup of such aggregates is a likely source of submicron particles.

Orbital debris from rocket exhaust and spacecraft materials is another possible source of submicron particles at high altitudes. We do not see a large concentration of almost pure alumina spheres that make up a major fraction of particles collected by aircraft, probably because the alumina

particles are typically tens of microns in size. However, it is possible that debris particles extend into the submicron range below the size that aircraft sampling is effective. Recent work by Zolensky et al. [36] has shown that while the concentration of IDP's has been constant over the period 1976–1984, collected orbital debris particles increased by a factor of 10. A portion of the excess particles that we have collected may be smaller debris particles at higher altitudes. A more complete answer must await a more thorough analysis of a large portion of the particles using TEM techniques.

The final potential source of submicron particles at the collection altitude is volcanic particles. The El Chichon volcanic event injected particles to between 33 and 35 km during 1982 [37]. Mackinnon et al. [31] surveyed particles collected by high altitude aircraft flown in 1982. Most of the volcanic particles consist of clusters of amorphous Al-rich silicate glass shards. Approximately 20% of the particles in the clusters were submicron. If submicron particles have sufficient residence time at our collection altitude they could represent a major fraction of our collected particles. Mackinnon et al. [31] calculated the time for irregularly shaped micron-sized particles to settle from 26 to 18 km, the aircraft collection altitude. For example, a 1 μm grain would take 10 years to settle this distance. Submicron particles at higher altitudes should show similar settling rates. Our collection probably contains a major portion of volcanic particles as well as extraterrestrial particles. The elemental data from the PIXE analysis and TEM analysis of the individual particles should be useful in resolving the origin of our collected particles.

Analysis of particles in the TEM is potentially the most comprehensive of the analytical techniques employed in that it allows morphological, elemental, and electron diffraction data to be obtained on individual particles. In Fig. 6 we see that the concentration of particles on the flight TEM grids is greater than the level of the handling blank (ASU Blank) that was run in parallel with the flight surfaces, but below the concentration of particles on the blanks that flew in the 1984 flight (LANL Blank). The particle levels on the LANL blank may be due to the long time in storage, contamination during ground handling of the payload, or atmospheric particles introduced by a leak in the seal plate and pump during the flight. Since we cannot distinguish between these possible sources of contamination, we assume that all of the particles are handling contamination. It should be noted, however that most of the particles on the blank grids consisted of carbonaceous particles while a majority of the particles on the flight grids were non-carbonaceous. The contamination level on the flight grids is not as severe as indicated simply by the particle counts on the blank grids.

The collected particles that were examined in detail generally fall into three classes based on their location in the Fe/Mg/Si ternary diagram in Fig. 8. One class is very low in Fe and Mg but high in Al relative to Si. These particles may be contaminates or volcanic particles, similar to the Al rich glass shards found by Mackinnon et al. [31], discussed above.

Another class of particles falls near the center of the diagram and show higher Mg and Fe concentrations relative to Al. Augite was identified in one of the particles (no. 9) in this group (Fig. 9). Although these particles fall in the general range of IDP's, individually they are by no means chondritic in composition. The wide scatter of particles in the diagram is expected relative to, for example, porous chondritic IDP's because these are much larger and tend to be multimineralic. Although a porous chondritic aggregate may be close to chondritic composition in bulk, the submicron particles that make up the aggregate vary widely in composition and mineralogy.

A third class of particles are those that are very high in Fe. An electron micrograph of one such particle (no. 22) is shown in Fig. 9. Troilite has been identified in this particle that has a very high Fe content. The origin of the iron-rich particles is not clear at present.

The elemental compositions of the particles in Table 1 show wide variations, frequently showing high concentrations of Cu and Zn. Some of the Cu signal may be an artifact from materials in the electron microscope. Cu and Zn are enriched in volcanic ash particles both from Mt. St. Helens [38] and El Chichon eruptions [39]. Pb and Cr also occur in high concentration in some of our particles. One of the particles is very high in Ba and S, perhaps from returning material from experi-

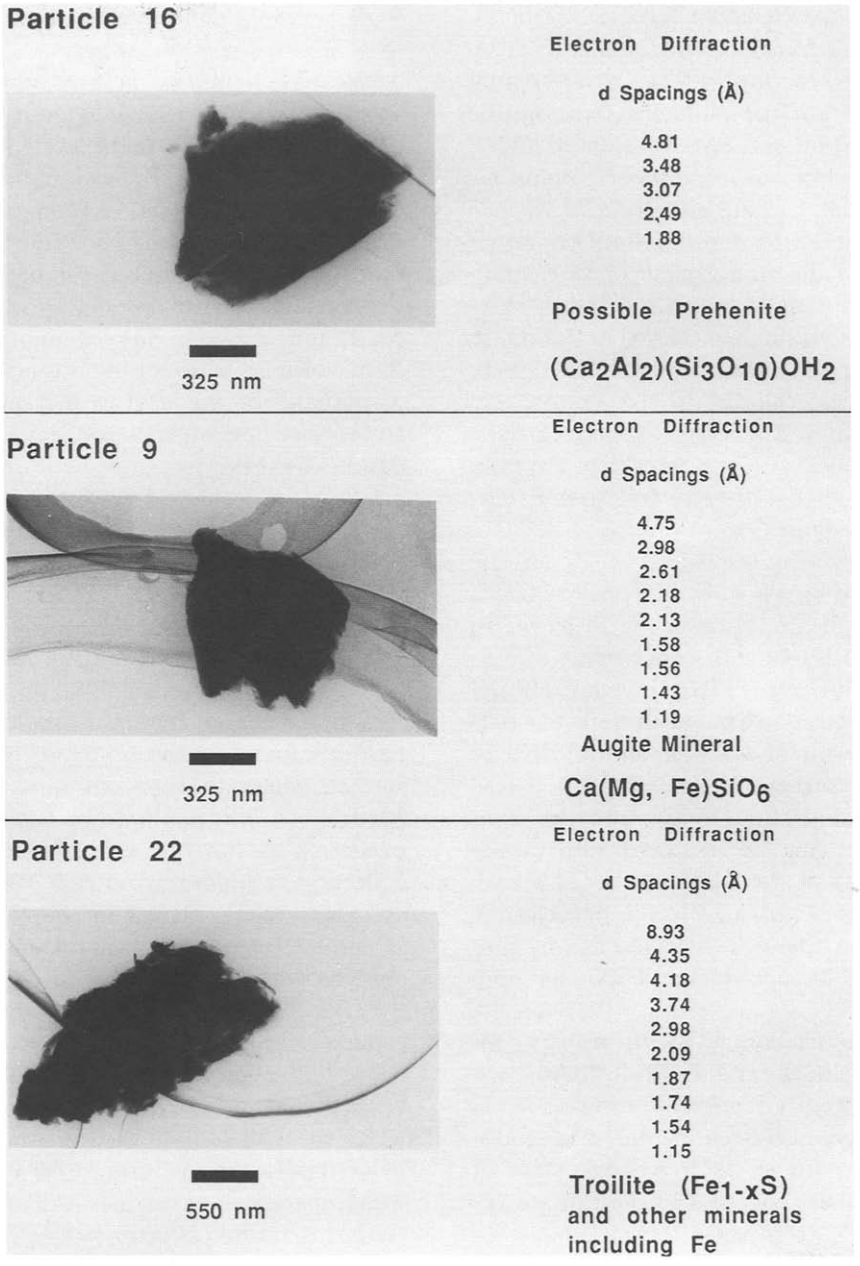

Fig. 9. Electron micrographs and electron diffraction data for selected particles from Fig. 8 and Table 1.

ments to study the earth's magnetosphere by releasing Ba [40], although Ba is enriched in volcanic ashes [41] and has been identified in IDP's [35]. Given the high contamination level on the grids and the dissimilarity with particles collected by aircraft we cannot positively identify the origin of the few particles that have been analyzed.

The PIXE data, taken at the center of the impact surface, should be substantially free from contamination since submicron particles dominate the collected mass in this area. Unfortunately only elements heavier than S could be detected, as noted above. Sulphur and chlorine are present in by far the highest concentrations, much greater

than expected if the elements occur as particles. We believe that Cl and S are predominantly from atmospheric gases reacting with the silver coating on the collection surface although some of the particles examined in the TEM also showed high S content, perhaps from absorption of sulphurous vapor species. Sulphur could also occur as sulphur rich droplets similar to those found on larger volcanic grains in the stratosphere or as calcium sulphate minerals [42]. Although the sulfur/chlorine ratio of 0.50 is higher than that found in seawater, including the mixing ratios of sulphate gases [43] and total chlorine in the stratosphere [44] one arrives at a S/Cl ratio similar to ours. The observed Ni/Fe ratio is greater than the ratio found in most terrestrial or extraterrestrial materials, but errors are large.

Relatively high concentrations of Br in the stratosphere noted by Vis et al. [45] are consistent with our data. High concentrations of Br have also been measured in IDP's with enrichments of 8 to 37 relative to Cl meteorites [46]. It is not clear if the Br that we detect is located in with the particles or is the result of reaction of stratospheric Br with the silver surface.

The high concentration of Cu and Zn is in agreement with finding Cu and Zn in some of the particles examined in the TEM. As noted above, Cu and Zn are enriched in volcanic particles. Sr and Zr have been found in volcanic ash in concentrations near 1000 ppm (Sr) and 100–200 ppm (Zr) [41].

The high concentration of Ti is surprising although both metallic Ti and Ti oxides have been found in IDP's from aircraft collections [35]. Ti and Fe oxides have also been identified in stratospheric volcanic particles [31]. A large class of stratospheric particles collected by aircraft are believed to originate from solid rocket exhaust or spacecraft debris [36]. Such particles show a wide variety of elements including Fe, Ni, Ti, Cu, and Zn.

Because of the wide composition ranges of possible particle sources, including volcanos, IDP's, and spacecraft, and the limited data available to date, we cannot assign an origin for the particles, even in the center of the impact surface where contamination is low. Further work needs to be done to measure the concentration of elements lighter than S either on the present particle collection or in future particle collections.

5. Conclusions and future work

We have collected a large number of stratospheric particles between 34 and 36 km that are unequivocally above blank levels for particle sizes between 0.045 and 1.0 μm radius. Our particle concentrations in this size range are orders of magnitude above the concentrations predicted by the model of Hunten et al. [9], but consistent with balloon and satellite observations. The higher concentration may be due to major contributions from volcanic particles, inaccuracies in the influx of particles of this size to the earth, breakup of larger particles, or high concentrations of orbital debris. We have not unequivocally identified the origin of the collected particles. However, only a small part of the collection has been examined in detail.

Future work can be divided into two areas; further analysis of the existing collection and analysis using improved analytical techniques on collections from future flights. In analysis of the present collection, emphasis needs to be placed on particles found at the center of the SEM impact surface where the concentration is the highest. Particle counting needs to be extended to smaller particle sizes. For future flights, refinement of the collection technique is needed. Particular emphasis needs to be placed on developing optimum substrates for particle counting, PIXE, and TEM analysis without extensive post-flight handling of the collected particles. Improved clean room procedures and clean balloon flight techniques are needed to allow confident sampling of particles larger than 1 μm in size. Advanced analytical techniques, including high resolution SEM and PIXE analysis in addition to the highly developed TEM analytical techniques will be invaluable in analyzing future collections.

Part of the difficulty in assigning origins to the particles is the uniqueness of our collected particles. Conventional stratospheric collections using aircraft sample the particle population below 20 km and collect only particles above about 1 μm. Typical IDP's are tens of μm in size. There are as yet no clear standards in the submicron range.

Acknowledgements

We acknowledge useful discussions with D. Brownlee, J. Bradley, G. Jessberger, F. Rietmeijer,

I. Mackinnon, and P. Buseck. We thank P. Buseck's group at Arizona State University for supporting the TEM analyses. We are grateful to D. McKay's group at Johnson Space Center and especially G. Nace for coating the beryllium grids. Early funding was provided by NASA Grant NAGW-210 and the Institute for Geophysics and Planetary Physics of the University of California and Los Alamos National Laboratory.

References

1 A. Adriani, G. Fiocco, G.P. Gobbi and F. Congeduti, Correlated behavior of the aerosol and ozone contents of the stratosphere after the El Chichon eruption, J. Geophys. Res. 92, 8365–8372, 1987.
2 P.V. Hobbs, J.P. Tuell, D.A. Hegg, L.F. Radke and M.W. Eltgroth, Particles and gases in the emissions from the 1980–1981 volcanic eruptions of Mt. St. Helens, J. Geophys. Res. 87, 11062–11066, 1982.
3 D.J. Hofmann and J.M. Rosen, On the temporal variation of stratospheric aerosol size and mass during the first 18 months following the 1982 eruptions of El Chichon, J. Geophys. Res. 89, 4883–4890, 1984.
4 A. D'Altorio and G. Visconti, Lidar observations of dust layers transcience in the stratosphere following the El Chichon volcanic eruption, Geophys. Res. Lett. 10, 27–30, 1983.
5 D.W. Hughes, Meteors, in: Cosmic Dust, J.A.M. McDonnell, ed., pp 123–186, J. Wiley, New York, N.Y., 1978.
6 G. Megie and J.E. Blamont, Laser sounding of atmospheric sodium; Interpretation in terms of global atmospheric parameters, Planet. Space Sci. 25, 1093–1109, 1977.
7 R.P. Turco, P. Hamil, O.B. Toon, R.C. Whitten and C.S. Kiang, A one-dimensional model describing aerosol formation and evolution in the stratosphere: I. physical processes and mathematical analogs, J. Atmos. Sci. 36, 699–717, 1979.
8 O.B. Toon, R.P. Turco, P. Hamil, C.S. Kiang and R.C. Whitten, A one-dimensional model describing aerosol formation and evolution in the stratosphere: II. sensitivity studies and comparison with observations, J. Atmos. Sci. 36, 718–736, 1979.
9 D.M. Hunten, R.P. Turco and O.B. Toon, Smoke and dust particles of meteoric origin in the mesosphere and stratosphere, J. Atmos. Sci. 32, 1342–1357, 1980.
10 F. Arnold and S. Qiu, Upper stratosphere negative Ion composition measurements and inferred trace gas abundances, Planet. Space Sci. 32, 169–177, 1984.
11 S. Qiu and F. Arnold, Stratospheric in situ measurements of H_2SO_4 and HSO_3 vapors during a volcanically active period, Planet. Space Sci. 32, 87–95, 1984.
12 D.E. Brownlee, Microparticle studies by sampling techniques, in: Cosmic Dust, J.A.M. McDonnell, ed., pp. 295–366, Wiley, New York, N.Y., 1978.
13 P.W. Hodge, ed., Interplanetary Dust, Gordon and Breach, New York, N.Y., 1981.
14 J.M. Rosen and D.J. Hofmann, Unusual behavior in the condensation nuclei concentration at 30 km, J. Geophys. Res., 88, 3725–3731, 1983.
15 S.V. Hering, R.C. Flagan and S.K. Friedlander, Design and evaluation of a new low-pressure Impactor. I., Environ. Sci. Technol. 12, 667–673, 1978.
16 F.J.M. Rietmeijer, A poorly graphitized carbon contaminant in studies of extraterrestrial materials, Meteoritics 20, 43–48, 1985.
17 P. Fraundorf, Interplanetary dust in the transmission electron microscope: diverse materials from the early solar system, Geochim. Cosmochim. Acta 45, 915–943, 1981.
18 M.B. Blanchard, D.E. Brownlee, T.E. Bunch, P.W. Hodge and F.T. Kayte, Meteoroid ablation spheres from deep-sea sediments, Earth Planetary Sci. Lett. 46, 178–190, 1980.
19 B. Mason, ed., Handbook of Elemental Abundances in Meteorites, Series on Extraterrestrial Chemistry, Gordon and Breach, New York, N.Y., 1971.
20 S.R. Taylor and S.M. McLennan, The Continental Crust: Its Composition and Evolution, Geoscience Texts, Blackwell, Oxford, 1985.
21 J.F. Luhr, I.S.E. Carmichael and J.C. Varekemp, The 1982 eruptions of El Chichon Volcano, Chiapas, Mexico: mineralogy and petrology of the Anhydrite bearing pumices, J. Volcanol. Geotherm. Res. 23, 69–108, 1984.
22 P.R. Kyle, P.E. Jezek, E. Mosley-Thompson and L.G. Thompson, Tephra layers in the Byrd Station ice core and the dome C ice core, Antarctica and their climatic importance, J. Volcanol. Geotherm. Res. 11, 29–39, 1984.
23 D. Twist and R.E.J. Harmer, Geochemistry of contrasting siliceous magmatic suites in the Bushveld discrimination diagrams, J. Volcanol. Geotherm. Res. 32, 83–98, 1987.
24 M.T. Osborn, J.M. Rosen, M.P. McCormick, P. Wang, J. Livingston and T.J. Swissler, SAGE II aerosol correlative observations: profile measurements, J. Geophys. Res. 94, 8353–8366, 1989.
25 P. Wang, M.P. McCormick, T.J. Swissler, M.T. Osborn, W.H. Fuller and G.K. Yue, Inference of stratospheric aerosol composition and size distribution from SAGE II satellite measurements, J. Geophys. Res., 94, 8435–8446, 1989.
26 J.M. Livingston and P.B. Russell, Retrieval of aerosol size distribution moments for multiwavelength particulate extinction measurements, J. Geophys. Res. 94, 8425–8433, 1989.
27 T.A. Cahill, Proton microprobes and particle-induced X-ray analytical systems, Annu. Rev. Nucl. Part. Sci. 30, 211–252, 1980.
28 N.A. Fuchs, The Mechanics of Aerosols, Pergamon, Oxford, 1964.
29 P. Meakin, Some recent advances in the simulation of diffusion limited aggregation and related processes, in: Fractals in Physics, L. Pietronero and E. Tosatti, eds., pp. 205–212, North Holland, New York, N.Y., 1986.
30 J.R. Stephens and B.K. Kothari, Laboratory analogues to cosmic dust, Moon Planets 19, 139–152, 1978.
31 I.D.R. Mackinnon, J.L. Gooding, D.S. McKay and U.S. Clanton, The El Chichon stratospheric cloud: solid particulates and settling rates, J. Volcanol. Geotherm. Res. 23, 125–146, 1984

32 G.S. Kent, M.C.W. Sandord and W. Keenliside, Laser radar observations of dust from comet Vennett, J. Atmos. Terr. Phys. 33, 1257–1262, 1971.
33 M.E. Zolensky and I.D.R. Mackinnon, Accurate stratospheric particles size distributions from a flat plate collection surface, J. Geophys. Res. 90, 5801–5808, 1985.
34 R.L. Hawkes and J. Jones, A quantitative model for the ablation of dust ball meteors, Mon. Not. R. Astron. Soc. 173, 339–356, 1975.
35 I.D.R. Mackinnon and F.J.M. Rietmeijer, Mineralogy of chondritic interplanetary dust particles, Rev. Geophys. 25, 1527–1533, 1987.
36 M.E. Zolensky, D.S. McKay and L.A. Kaczor, A tenfold increase in the abundance of large solid particles in the stratosphere, as measured over the period 1976–1984, J. Geophys. Res. 94, 1047–1056, 1989.
37 K.E. Coulson, T.E. Defour and J. Deluis, LIDAR and optical polarization measurements of stratospheric cloud in Hawaii, EOS, Trans. Am. Geophys. Union, 63, p. 897, 1982.
38 E. Thomas, J.C. Varekamp and P.R. Buseck, Zinc enrichment in the phreatic ashes of Mt. St. Helens, April 1980, J. Volcanol. Geotherm. Res. 12, 339–350, 1982.
39 D.C. Woods and R.L. Chuan, Size-specific composition of aerosols in the El Chichon volcanic cloud, Geophys. Res. Lett. 10, 1041–1044, 1983.
40 M.W. Dunlop, D.J. Southwood, R.P. Rijnbeek, W.A.C. Mier-Jedrzejowicz and M.A. Saunders, Magnetic stresses during the solar wind barium release on 27 December 1984, in: Solar Wind Interactions, Proceedings of Symposium 6 of the COSPAR 26th Plenary Meeting, Toulouse, Adv. Space Res. 6, 185–190, 1986.
41 J.C. Varekamp, J.F. Luhr and K.L. Prestegaard, The 1982 eruptions of El Chichon volcano (Chiapas, Mexico): character of the eruptions, ash fall deposits and gas-phase, J. Volcanol. Geotherm. Res. 23, 39–68, 1984.
42 I.D.R. Mackinnon and D.W. Mogk, Surface sulfur measurements on stratospheric particles, Geophys. Res. Lett. 12, 93–96, 1985.
43 F. Arnold and R. Fabian, First measurements of gas phase sulphuric acid in the stratosphere, Nature 283, 55–57, 1980.
44 R. Gammon, Tropospheric trace gases: sources, distributions, and trends in: Global Ozone Research and Monitoring Project, pp. 57–116, World Meteorol. Org. Rep. 16, Geneva, 1985.
45 R.D. Vis, C.C.A.H. van der Stap and D. Heymann, On the use of a nuclear microprobe for trace element analysis in meteorites and cosmic dust, Nucl. Instrum. Methods Phys. Res. 22, 380–385, 1987.
46 S.R. Sutton and G.J. Flynn, Extraterrestrial volatiles in the stratosphere, Proceedings of the XIX Lunar and Planetary Science Conference, p. 1155, 1988.